JOURNAL OF AIRCRAFT
Vol. 42, No. 6, November–December 2005

Effect of Camber on the Aerodynamics of Adaptive-Wing Micro Air Vehicles

W. Null* and S. Shkarayev†
University of Arizona, Tucson, Arizona 85721

Four microair vehicle wind-tunnel models were built with 3, 6, 9, and 12% camber, all based upon the S5010-TOP24C-REF thin, cambered-plate airfoil. These models were tested in the Low Speed Wind Tunnel at angles of attack ranging from 0 to 35 deg and velocities of 5, 7.5, and 10 m/s, corresponding to mean aerodynamic chord Reynolds numbers of 5×10^4, 7.5×10^4, and 1×10^5, respectively. Aerodynamic coefficients C_L, C_D, C_M and lift-to-drag ratio (L/D) were obtained and plotted vs angle of attack for all of the cambers at each velocity. Large positive, nose-up pitching moment coefficients were found with all cambers at the lowest Reynolds number. These results have been verified with flight tests of micro air vehicles utilizing these airfoils. The 3% camber wing gives the best lift-to-drag ratio of the four cambers and theoretically would be the optimal choice for high-speed, efficient flight. It is theorized that the 6 and 9% camber wings will give the best low-speed performance because of their high lift-to-drag ratios and mild pitching moments near their stall angles of attack.

Nomenclature

A	=	aspect ratio (b^2/S)
b	=	wing span
C_D	=	drag coefficient, $= D/(0.5\rho V^2 S)$
C_L	=	lift coefficient, $= L/(0.5\rho V^2 S)$
$C_{L\max}$	=	maximum lift coefficient
C_{L_α}	=	lift-curve slope (1/deg)
C_M	=	quarter-chord pitching-moment coefficient, $= M/(0.5\rho V^2 S\bar{c})$
c	=	root chord measured along the longitudinal axis of the wing
$\bar{c}$	=	mean aerodynamic chord measured along the longitudinal axis of the wing
D	=	drag force
d	=	position of maximum reflex
h	=	height of maximum camber
h_i	=	height of inverse camber
L	=	lift force
M	=	pitching moment about quarter-chord point of the root chord
Re	=	Reynolds number
t	=	thickness of the wing
V	=	freestream velocity
α	=	angle of attack, deg
ρ	=	air density

Introduction

IN 1996 the Defense Advanced Research Projects Agency (DARPA) initiated a broadly based program initiative on micro air vehicles. The main purpose of the DARPA Micro Air Vehicle (MAV) Program was to determine if evolving technologies (i.e., miniature electronics, propulsion systems, wireless video systems, etc.) could be integrated into a small, unmanned aircraft capable of reliably performing basic military surveillance and reconnaissance.[1] In addition to their envisioned military role, MAVs could also be beneficial to law enforcement agencies, search and rescue personnel, as well as news agencies, city planners, real estate brokers, and more.

It is easy to see why the military is so enthusiastic about MAV technology coming to fruition. With an MAV in his pack, a soldier could fly the craft out over enemy-occupied territory, gathering vital, real-time information that could lead to the success of a campaign as well as sustaining the overall health of his platoon. This basic reconnaissance could be achieved cheaply, quickly, and safely with a mission-capable MAV. In addition to providing basic reconnaissance and surveillance, MAVs could be equipped with sensors to help locate munitions or to conduct nighttime surveillance, all with a craft so small that it would go virtually unnoticed.

In recent years there has been a concerted effort to try to determine the optimum airfoil configuration for these low Reynolds number Re flight vehicles (low Reynolds number is assumed to be less than 2×10^5). Aerodynamic data for traditional airfoils, such as the NACA series, are available in catalog.[2] It is apparent from the presented data that the aerodynamics of traditional airfoils suffers greatly at these low speeds and lift-to-drag ratio significantly decreases with a Reynolds number decrease. Experimental measurements in wind tunnels at the low-Reynolds-number regime become difficult because aerodynamic forces are small at low angles of attack, requiring high measuring accuracy and sensitivity. Selig et al.[3] developed an inverse computational approach for designing airfoils, providing the designer an effective tool for achieving desired aerodynamic performance. Using this approach, several series of low-Reynolds-number airfoils were created and validated through wind tunnel testing.

A valuable collection of papers regarding MAV aerodynamics is presented in Ref. 4, and it is one of the most complete works on MAV aerodynamics to date. However, even today with the abundance of knowledge regarding MAVs, more research is needed, particularly in the area of wing optimization for the different phases of MAV flight (i.e., ingress/egress and loiter).

In the wind tunnel testing conducted by Schmitz,[5] model wings of rectangular planform, with aspect ratios of 5 were tested in the range from $Re = 2 \times 10^4$ to 1.7×10^5. A 12% maximum thickness wing, 2.9% thickness flat plate (0% camber), and cambered (5.8% camber) plate were investigated. It was discovered that at Reynolds numbers around 4.2×10^4, the maximum lift coefficient of a thin, cambered-plate wing ($C_{L\max} = 1.05$) was nearly twice that obtained for a traditional 12% thickness wing. Results of this study demonstrated the superiority of the thin, cambered wing for use in the low-Re regime.

Presented as Paper 2004-2694 at the AIAA 2nd Flow Control Conference, Portland, OR, 28 June–1 July 2004; received 24 July 2004; revision received 2 December 2004; accepted for publication 3 February 2005.

*Graduate Research Assistant, Department of Aerospace and Mechanical Engineering, 1130 N. Mountain Avenue. Member AIAA.

†Assistant Professor, Department of Aerospace and Mechanical Engineering, 1130 N. Mountain Avenue; svs@email.arizona.edu. Senior Member AIAA.

These data, although limited to one cambered-plate wing, paved the way for further research into the benefits of cambered-plate wings at low Reynolds numbers.

Laitone[6,7] studied rectangular wings with aspect ratios of 5 for $Re = 2 \times 10^4$ to 7×10^4. Results of these studies supported the conclusions of the study[5] that a 5% circular arc, 1% thick cambered wing produced the highest lift-to-drag ratio and highest $C_{L\max}$. Test results[8] for a circular flat disk (aspect ratio $A = 4/\pi$) at $Re = 5 \times 10^4$ were very promising, as they compared well with square and delta wings of $A = 1$.

Pelletier and Mueller[9] conducted a series of low-Re tests of thin flat-plate and cambered-plate wings of low aspect ratios. Test models were of rectangular planform. Both flat plates as well as various 4%, circular-arc cambered-plate wings were tested, all of approximately 2% thickness. This work showed that the cambered-plate wings outperformed the flat plates and interestingly enough, found that the hysteresis inherent in the lift curves of traditional wings at low Reynolds numbers was virtually nonexistent in the thin plates.

Torres and Mueller[10] studied the effect of wing planform and aspect ratio on the lift and drag of flat plates of thickness-to-chord ratio 1.96% and of aspect ratios 0.5, 1.0, and 2.0 that were tested for $Re = 7 \times 10^4$ to 1.4×10^5. It was found that for $A \leq 1$ the rectangular and inverse Zimmerman planforms had advantages over Zimmerman or elliptical planforms.

The wing loading of MAVs needs to be low (less than approximately 13 oz/ft^2 (38.9 N/m^2) for a vehicle of this scale) in order to provide adequate controllability. The design constraint on the maximum dimension of MAVs can dictate the selection of a circular planform, giving a maximum wing area for a given maximum dimension. For the same reason, many MAVs utilize a flying wing configuration. The biggest factor driving the design of the flying wing aircraft is pitch stability and control. Except for the work of Pelletier and Mueller,[9] previous studies have not provided data on pitching moment coefficients. Large negative, nose-down pitching moment coefficients were found for cambered, low-aspect-ratio wings at the low Reynolds number.[9] This moment can be compensated for by introducing a wing with inverse camber (reflexed camber).

Past work by the authors has resulted in some interesting findings regarding the benefits of micro air vehicles utilizing adaptive wings.[11,12] In Ref. 11 the concept of an adaptive-wing micro air vehicle (with an emphasis on variable camber) was introduced, and a flying test model was developed that was capable of camber change from 0% (flat plate) to approximately 9%. Test flights were made with this vehicle demonstrating the flight speed variation by inducing a simple camber change.

In Ref. 12 a series of wind-tunnel tests were conducted on wind-tunnel models varying from 3 to 12% camber. The Selig 5010 (S5010) flying wing airfoil[13] was used as a baseline for the design of a thin, cambered-plate airfoil. The standard S5010 airfoil has 5% camber and a thickness of 10%. The top surface of the S5010 was used as a starting point for the thin, cambered-plate airfoil design. The modified airfoil was renamed to S5010-TOP24C. The wind-tunnel models used in this previous series of tests were complete with fuselages and represented as close as possible the actual MAV flight vehicles designed by researchers at the University of Arizona. Motor/propeller tests were also conducted to determine the dynamic thrust characteristics of the propulsion system. With the results of these tests analyzed, it was determined that the flight speed of the MAV could theoretically be increased or decreased by as much as 25% via camber change with virtually no increase in power consumption.

Although the aforementioned series of tests provided some information regarding the benefits of variable camber on the model in question, the true nature of the wing-only characteristics was somewhat masked because a fuselage was implemented during the testing. On a vehicle of this scale (~8-in. chord), the fuselage covered over 25% of the lower surface of the wing and likely contributed to some unsteady aerodynamics that could significantly affect the overall results of the change in airfoil camber.

Therefore the purpose of this series of testing was to precisely determine the behavior of C_L, C_D, and C_M (the lift, drag, and quarter-chord pitching moment coefficients, respectively) with a change in camber of the *wing only* for different Reynolds numbers.

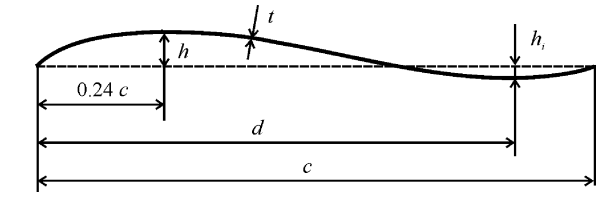

Fig. 1 S5010-TOP24C-REF airfoil used in this series of wind-tunnel tests.

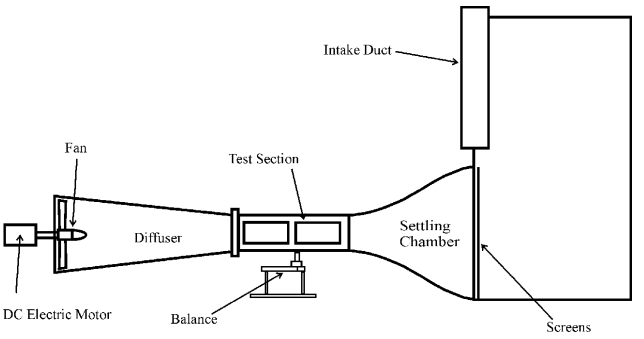

Fig. 2 Schematic of the Low Speed Wind Tunnel.

Experimental Facility, Models and Methods

The airfoil used in this series of tests is named S5010-TOP24C-REF (see Fig. 1) and represents an increased reflex version of the airfoil section used in the previous study.[12] The increased reflex was added after numerous test flights showed that MAVs utilizing the preceding airfoil section needed excessive up-elevator deflections to maintain steady, level flight, resulting in decreased flight times.[14]

The facility used to perform this series of tests is known as the Low Speed Wind Tunnel and is located in the Department of Aerospace and Mechanical Engineering at the University of Arizona. The tunnel is a suction-based, nonreturn tunnel with a test section of 4×3 ft (1.2×0.9 m) and is capable of speeds from 2 to 50 m/s. The wind tunnel is rated at a 0.3% turbulence level in the axial direction for the freestream velocities used in the present study. A schematic of the tunnel is seen in Fig. 2.

The force-balance system contains six precision strain gauges for measuring lift, drag, side force, pitching, rolling, and yawing moments. For this sequence of tests, no side forces were analyzed because the models were symmetrical and rolling and/or yawing moments were not sought.

The data acquisition system (DAQ) utilizes a National Instruments low-noise SCXI-1000 chassis that is capable of sampling rates up to 333,000 samples per second for each DAQ device. The acquisition devices themselves are two National Instruments SCXI-1321 terminal blocks. National Instruments LabView 6.0 software provides the user interface and is used for sampling the data from the DAQ devices and permanently writing the sampled data to a Microsoft Excel spreadsheet for later aerodynamic analysis. The resolution of the DAQ is 16 bits.

Four wind tunnel models were built with 3, 6, 9, and 12% camber, all based upon the S5010-TOP24C-REF airfoil mentioned earlier. The 6% camber S5010-TOP24C-REF airfoil is shown in Fig. 1. The construction of the wing shape for this current study was performed in the following manner: first, an S5010-TOP24C-REF airfoil (Fig. 1) of constant 8.125-in chord was swept in the spanwise direction to form a constant chord rectangular wing section. Then, the circular planform (with squared-off leading edge) as shown in Fig. 3 was projected onto the rectangular wing surface to form the complete wing planform and profile. All wings had the same chord length c, wing area S, and thickness t. The relative thickness of the airfoil is $t/c \approx 0.25\%$. The leading edge was rounded with a

Table 1 Wind-tunnel model wing geometry

Camber, %	3	6	9	12
Wing area S, in.^{2}	60	60	60	60
Chord length c, in.	8.125	8.125	8.125	8.125
Camber height h, in.	0.244	0.488	0.731	0.975
Thickness t, in.	0.02	0.02	0.02	0.02
Position of maximum reflex d, in.	7.312	7.062	7.000	6.937
Inverse camber h_i, in.	0.094	0.187	0.250	0.375

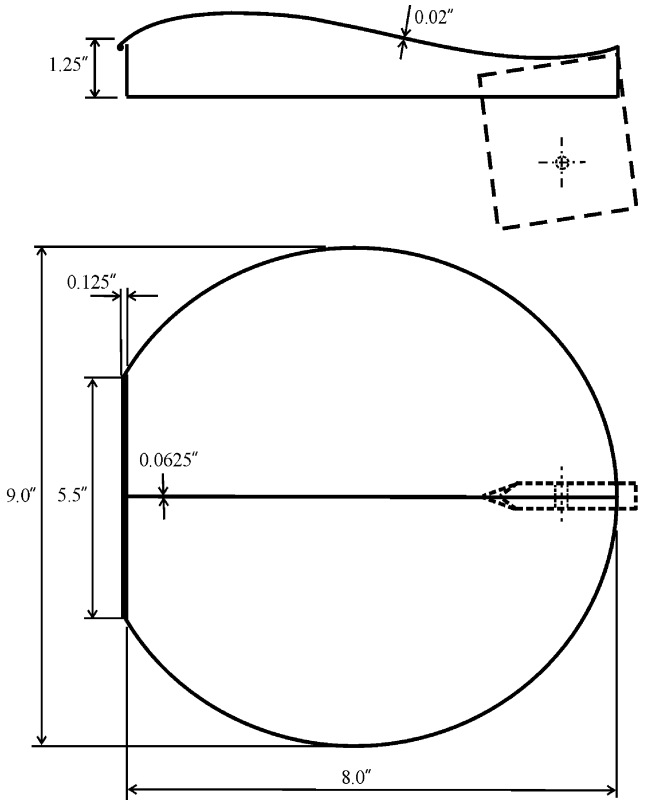

Fig. 3 Representative MAV wind-tunnel model and mount (– – – –).

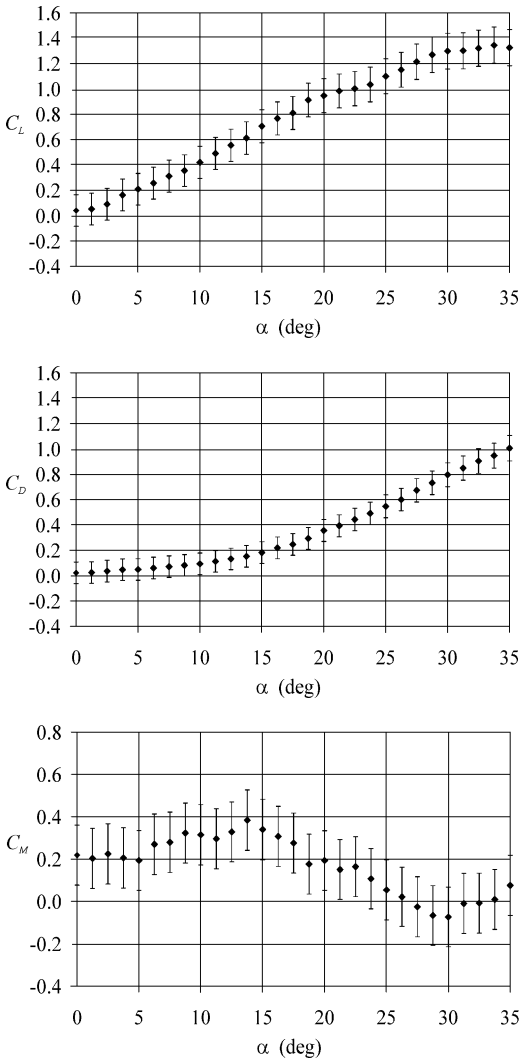

Fig. 4 Aerodynamic coefficients with error bars for 3% camber wing at $Re = 5 \times 10^4$.

0.0625-in. radius. The rest of the wing data can be found in Table 1. A very significant feature of these designed wings is that the ratio of inverse camber to regular camber is $h_i/h \approx 1/3$.

The wings were constructed with one layer of 6-oz/ft^2 carbon-fiber cloth laminated with epoxy resin. The resulting carbon wing has a thickness of approximately 0.02 in. and $t/c = 0.246\%$. A carbon-fiber tube of 1/8-in.-diam was then bonded to the leading edge of each wing to produce a smooth, rounded leading edge. Because the main goal of this testing series was to obtain wing-only aerodynamic data, it was decided that the wing would be mounted in the wind tunnel as close to the trailing edge as possible and with an "aerodynamically clean" mount system. An aluminum mount was constructed with minimum frontal area and with a smooth, aerodynamic leading edge. Because the wing would be mounted near the trailing edge, the wing was made stiffer by bonding a 1/16-in. plywood "rib" from the leading to the trailing edge. This rib also functioned as the mounting point for the wind tunnel mount. A schematic of a representative wind tunnel model is seen in Fig. 3.

Each model was mounted in the wind tunnel and tested at velocities of 5, 7.5, and 10 m/s, corresponding to chord Reynolds numbers of 5×10^4, 7.5×10^4, and 1×10^5, respectively. Angles of attack ranged from 0 to 35 deg in increments of 1.66 deg per data point. Using the raw wind tunnel data as well as the model geometry, plots of the lift, drag, and pitching moment coefficients about the quarter-chord point were computed for each camber and for each Reynolds number.

Test Results

To determine the error in the measured aerodynamic coefficients, a calibration of the wind tunnel and the balance was performed before each test series. Following procedures described in Ref. 15, standard deviations of lift, drag, pitching moment, and dynamic pressure were estimated. Plots of the aerodynamic coefficients C_L, C_D, and C_M for 3% camber wing at $Re = 5 \times 10^4$ are shown in Fig. 4. Utilizing calibration measurements[15] and the small-sample method,[16] the uncertainty intervals in aerodynamic coefficients corresponding to a confidence level of 99% were determined and error bars plotted in Fig. 4. Solid blockage, wake blockage, and streamlined curvature corrections were estimated based on the methods described in Ref. 17 and found negligible.

Plots of the aerodynamic coefficients for the 3% camber ($Re = 7.5 \times 10^4$ and 1×10^5), 6, 9, and 12% cambers ($Re = 5 \times 10^4$, 7.5×10^4, and 1×10^5) can be seen in Figs. 5–8, respectively. From the plots of all cambers, it is noticeable that the pitching moment coefficient about the quarter-chord point C_M is highest (in the positive, nose-up direction) at the lowest of the Reynolds number values tested. This phenomenon has been seen during flight tests of MAVs implementing these wings; during slow-flight maneuvers (less than 5 m/s), the nose of the aircraft tends to rotate upwards toward the stall point and requires downelevator control surface inputs from the pilot to keep the aircraft from stalling. At higher flight speeds this phenomenon has not been seen, and it is interesting to see that the wind tunnel data and the flight test observations seem to correlate.

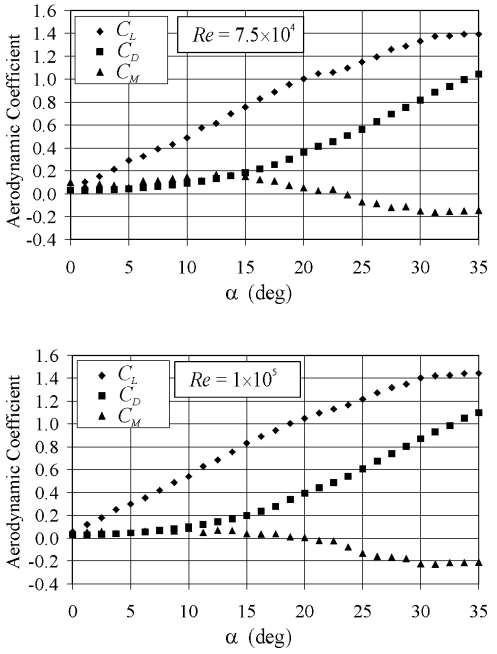

Fig. 5 Aerodynamic coefficients for 3% camber wing at $Re = 7.5 \times 10^4$ and 1×10^5.

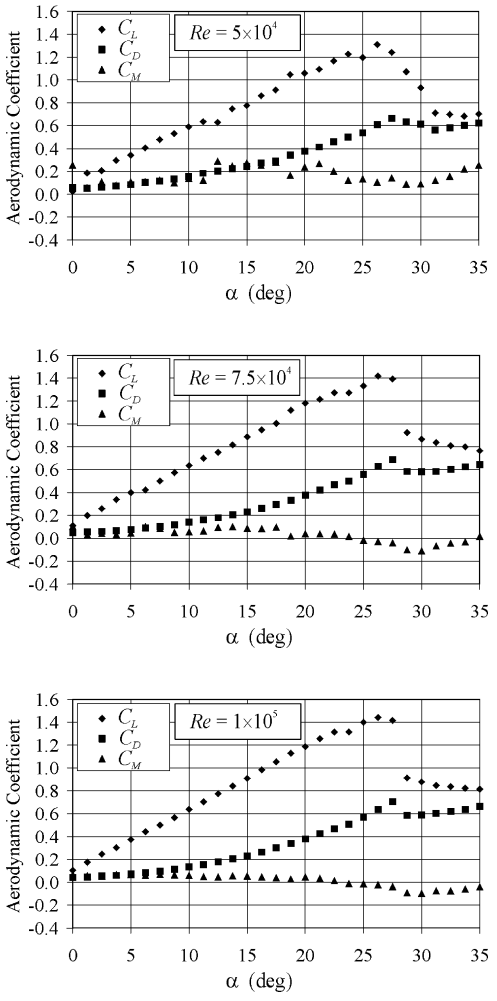

Fig. 6 Aerodynamic coefficients for 6% camber wing at $Re = 5 \times 10^4$, 7.5×10^4, and 1×10^5.

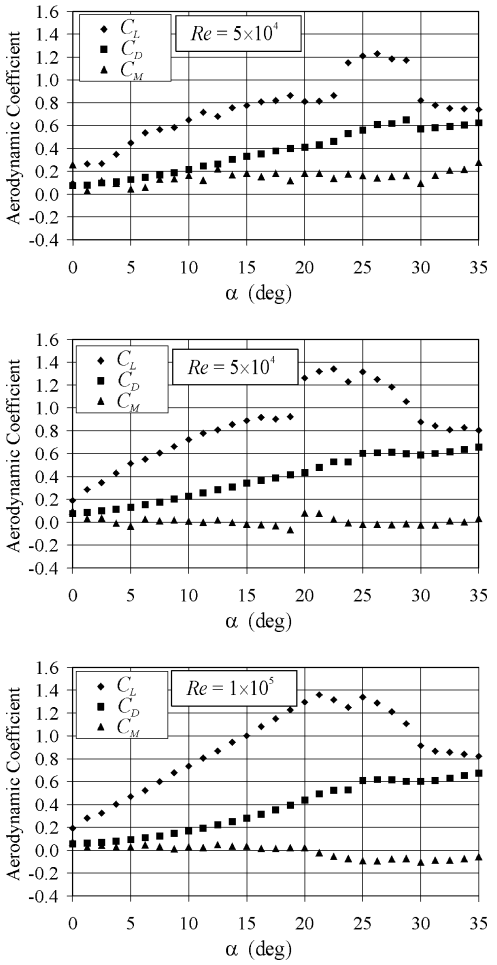

Fig. 7 Aerodynamic coefficients for 9% camber wing at $Re = 5 \times 10^4$, 7.5×10^4, and 1×10^5.

Discussion of Results

The lift-to-drag ratio is typically one of the greatest performance measures when it comes to choosing or designing a wing for virtually any flight vehicle. Micro air vehicles are no exception, and in fact are likely more adversely affected by low L/Ds. With their inherently low aspect ratios (typically less than 2.0) and low-Reynolds-number flight environment, MAVs utilizing inefficient airfoil sections (poor lift-to-drag ratios) are doomed to be poor performers with reduced endurance, low climb rates, and slow flight speeds.

Plots of the lift-to-drag ratios of the four different cambers tested in this series clearly point to the best performing camber, at least when it comes to high speed flight efficiency. It is seen in Fig. 9 that the 3% camber wing by far surpasses even the 6% camber when it comes to this measure of performance. With a L/D of over 6.5 at an Re of 1×10^5, it easily surpasses the 6% camber, the next contender, by a margin of almost 25%. The poorest performer is also easily seen; the 12% camber wing has a maximum lift-to-drag ratio of below 3.0 at all Reynolds number values. In fact, the L/D data points of the 12% camber are nearly on top of each other for all tunnel velocities. It would be interesting to test the higher cambers at even lower Reynolds number values to see if the same trend continues.

The lift curves are typically one of the first things to look at when analyzing aerodynamic data. Plots of the lift curves can be seen in Fig. 10. The slopes of the lift curves were calculated with the help of a least-square linear regression and presented in the Table 2. Only data corresponding to the angle of attack from 1.25 to 10 deg were kept in calculations. Table 2 shows the increasing values of C_{L_α} with an increase of Reynolds number. C_{L_α} also increases as the wing camber increases from 3 to 9%, but then drops at 12%.

It is interesting to see from Fig. 10 that the 3% camber wing does not show the typical, abrupt stall seen with the 6 and 9% cambers,

Table 2 Lift-curve slopes

Camber, %	3	6	9	12
$Re = 5 \times 10^4$	0.041	0.048	0.049	0.024
$Re = 7.5 \times 10^4$	0.045	0.049	0.050	0.029
$Re = 1 \times 10^5$	0.048	0.052	0.053	0.033

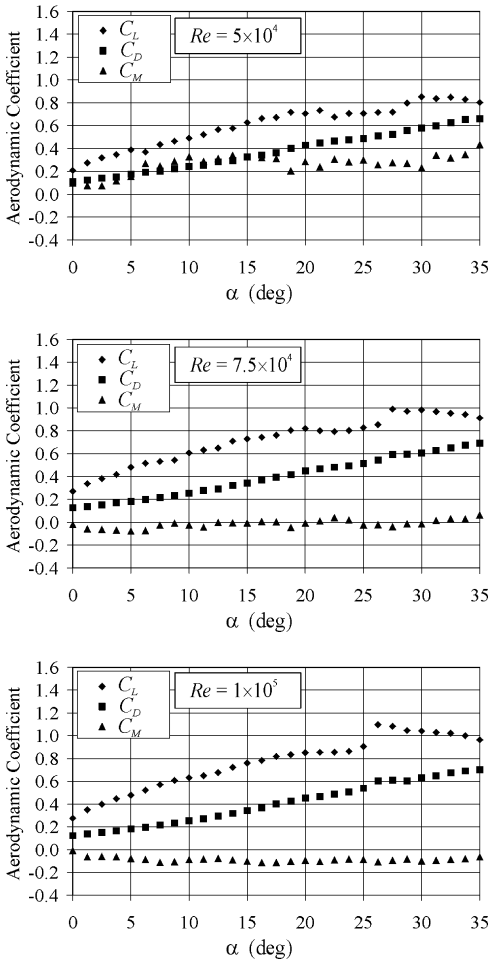

Fig. 8 Aerodynamic coefficients for 12% camber wing at $Re = 5 \times 10^4$, 7.5×10^4, and 1×10^5.

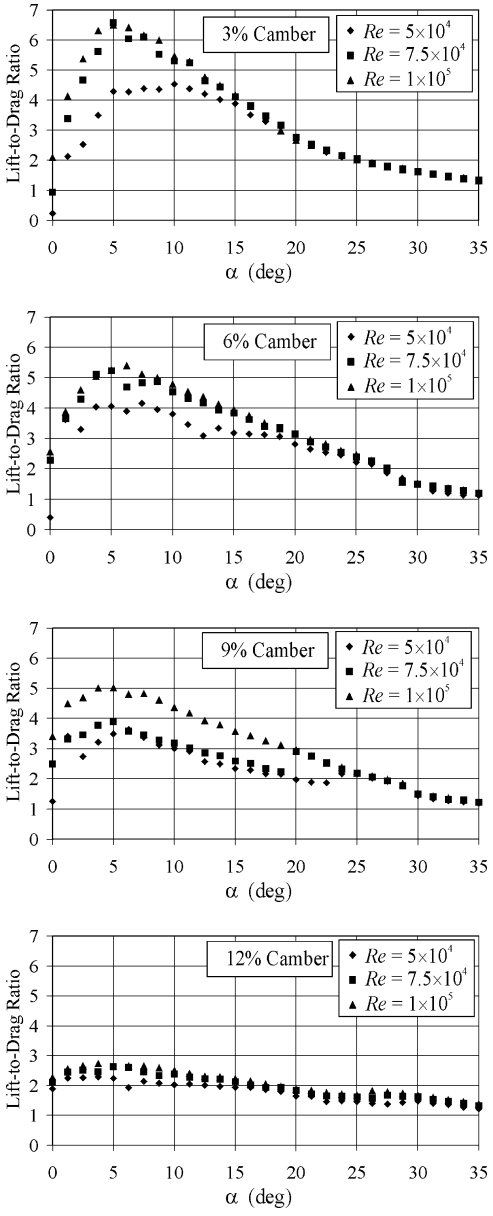

Fig. 9 Variation of *L/D* with Reynolds number.

and somewhat with the 12% camber (the 12% camber at the highest Reynolds number somewhat of a lift "spike" near where the stall point would be expected to be). Showing somewhat strange lift-curve behavior is the 9% camber wing. From the plots of the two lower Reynolds numbers, there are strange spikes in the lift curves in the range of 20- to 23-deg angle of attack. At first it was thought that errors occurred during testing, and so the tests were repeated. The repeated tests showed the exact same behavior as the first tests so the phenomena are assumed to be real. It is unclear what is causing the lift spikes. From the appearance of the lift curves of the 3% camber wing, it seems that it would be a very good wing to use on a micro air vehicle model because of the predictability of the lift characteristics coupled with the high lift-to-drag ratios. Although the hysteresis of the lift curves was not studied in this series of tests, it would be highly beneficial for a future study.

In terms of trends, it appears that as the camber increases the stall angle of attack decreases. Looking closely at Fig. 10, it appears that the stall angle of attack of the 3, 6, and 9% cambers are at approximately 33, 27, and 25 deg, respectively. Of interest is that the 3% camber wing does not show a true stall while the 12% camber shows a dramatically reduced lift-curve slope with a lift spike/stall somewhere in the range of 26-deg angle of attack. It is unclear what is causing the erratic lift-curve behavior in the 12% camber.

In terms of slow speed flight, it appears that the 6 and 9% camber wings can give the best performance, showing nearly identical behavior. This was determined from analyzing the lift-to-drag and pitching-moment plots; the 6 and 9% camber wings give excellent lift-to-drag ratios at their stall angles of attack with only mild nose-up pitching moments: L/D of approximately 2.1 at the stall angles of attack of approximately 25 deg. These results are followed by the 3 and 12% cambers.

A comparison of the data for the 6% camber with that obtained from study[18] on a similar wing of 6.5% camber shows excellent correlation at $Re = 7.5 \times 10^4$ and 10^4. In the previous research[18] it was found that the lift curve slope $C_{L_\alpha} = 0.05$ is very close to the values of C_{L_α} presented in the Table 2 for the 6% camber. In addition, the research[18] shows a maximum lift coefficient of approximately 1.4 at a Reynolds number of 7×10^4 while the current research shows a maximum lift coefficient of 1.42 at a Reynolds number of 7.5×10^4. Finally, wind-tunnel test results[8] for the flat circular disk (aspect ratio $A = 4/\pi$) at $Re = 5 \times 10^4$ were $C_{L_\alpha} = 0.044$ and $C_{L\max} = 1.44$ at $\alpha = 35$ deg. These numbers are in a very good agreement with the results obtained in the present study for the wing with 3% camber: $C_{L_\alpha} = 0.041$ and $C_{L\max} = 1.34$ at $\alpha = 34$ deg. It was expected that these results should be in good agreement with the flat circular disk because the planform shapes are nearly identical and that the 3%

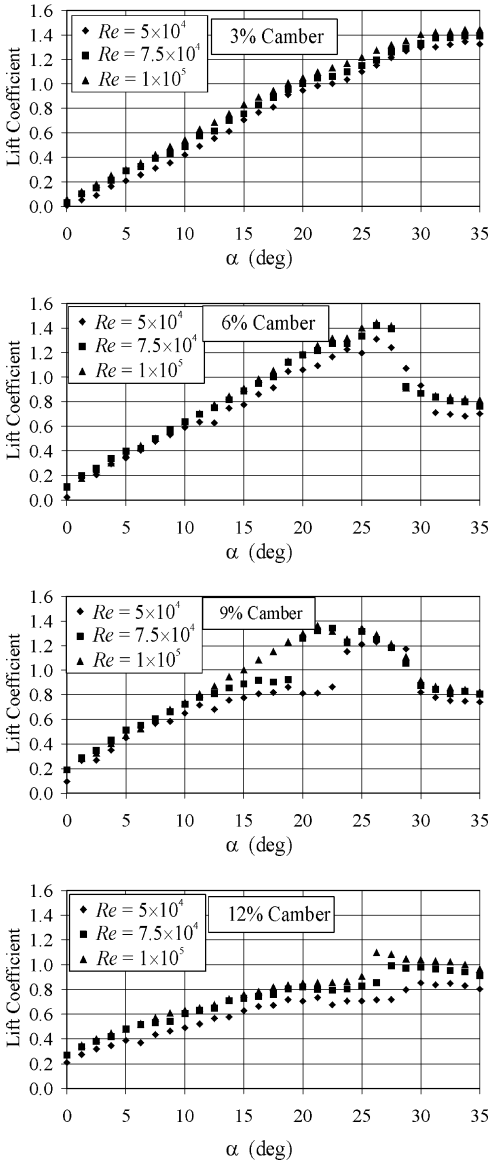

Fig. 10 Variation of lift coefficient with Reynolds number.

camber wing used in the present study is the closest approximation to a flat plate.

Conclusions

There is a need for the design of small flying wings with thin, cambered-plate wings that deliver adequate performance in the low-Reynolds-number flight regime. From analyzing the wind-tunnel data obtained in the present study, it appears that for wings with a circular planform the 3–9% cambers give the best range of performance of the four cambers tested. Results from the 12% camber were less promising, both from a lift-to-drag standpoint as well as a lift-curve standpoint.

For high-speed flight (i.e., ingress/egress for a typical MAV mission) it appears that the 3% camber wing will give the best performance because of its high lift-to-drag ratio of over 6.5. To fly at this angle of attack would likely require a substantial flight speed, which might make control of the MAV more difficult. For slow speed flight, as in a loiter situation, it appears that the 6 and 9% cambers will perform the best, showing nearly identical performance. In looking at the stall angle of attacks for each wing, the 6 and 9% camber wings have the highest, nearly identical lift-to-drag ratios at their stall angles of attack compared to the other two cambers. These wings are followed in theoretical slow flight performance by the 3 and 12% cambers, respectively.

In the next series of tests, the influence of the motor/propeller combination will be studied in the hopes of determining the exact role that propulsive-induced lift acts, particularly at high angles of attack. This will add more needed information for a low-speed flight analysis.

Acknowledgments

The authors would like to acknowledge with pleasure the discussions and suggestions from Martin R. Waszak of NASA Langley Research Center. This research was sponsored by NASA Langley Research Center under Grant NAG-1-03045. The authors also acknowledge Frank Champagne and Luis Willis for their help in obtaining the wind-tunnel data.

References

[1]McMichael, J. M., and Francis, M. S., "Micro Air Vehicles—Toward a New Dimension in Flight," Defense Advanced Research Projects Agency, TTO Document, Washington, DC, 7 Aug. 1997, URL: http://www.darpa.mil/tto/mav/mav_auvsi.html [cited 12 July 2004].

[2]Miley, S. J., "A Catalog of Low Reynolds Number Airfoil Data for Wind Turbine Applications," Rockwell International, U.S. Dept. of Energy, Wind Energy Technology Div., Texas A&M Univ., Federal Wind Energy Program, RFP-3387, UC-60, College Station, TX, Feb. 1982.

[3]Selig, M. S., Gopalarathnam, A., Giguère, P., and Lyon, C. A., "Systematic Airfoil Design Studies at Low Reynolds Numbers," *Fixed and Flapping Wing Aerodynamics for Micro Air Vehicle Applications*, edited by T. J. Mueller, Vol. 195, AIAA, Reston, VA, 2001, pp. 143–167.

[4]Mueller T. J. (ed.), *Fixed and Flapping Wing Aerodynamics for Micro Air Vehicle Applications*, Progress in Aeronautics and Astronautics, Vol. 195, AIAA, Reston, VA, 2001, p. 586.

[5]Schmitz, F. W., "Aerodynamics of the Model Airplane. Part I. Airfoil Measurements," 1941, Redstone Arsenal Translation, RSIC-721, Huntsville, AL, 22 Nov. 1967.

[6]Laitone, E. V., "Wind Tunnel Tests of Wings at Reynolds Numbers Below 70000," *Experiments in Fluids*, Vol. 23, No. 5, 1997, pp. 405–409.

[7]Laitone, E. V., "Aerodynamic Lift at Reynolds Numbers Below 7×10^4," *AIAA Journal*, Vol. 34, No. 9, 1996, pp. 1941, 1942.

[8]Laitone, E. V., "Wind Tunnel Tests of Wings and Rings at Low Reynolds Numbers," *Fixed and Flapping Wing Aerodynamics for Micro Air Vehicle Applications*, edited by T. J. Mueller, Vol. 195, AIAA, Reston, VA, 2001, pp. 83–90.

[9]Pelletier, A., and Mueller, T. J., "Low Reynolds Number Aerodynamics of Low-Aspect-Ratio, Thin/Flat/Cambered-Plate Wings," *Journal of Aircraft*, Vol. 37, No. 5, 2000, pp. 825–832.

[10]Torres, G. E., and Mueller, T. J., "Aerodynamic Characteristics of Low Aspect Ratio Wings at Low Reynolds Numbers," *Fixed and Flapping Wing Aerodynamics for Micro Air Vehicle Applications*, edited by T. J. Mueller, Vol. 195, AIAA, Reston, VA, 2001, pp. 115–141.

[11]Null, W., Wagner, M., Shkarayev, S., Jouse, W., and Brock, K., "Utilizing Adaptive Wing Technology in the Control of a Micro Air Vehicle," *Smart Structures and Materials 2002: Industrial and Commercial Applications of Smart Structures Technologies*, edited by Anna-Maria R. McGowan, Proceedings of SPIE, Vol. 4698, International Society for Optical Engineering, Bellingham, WA, 2002, pp. 112–120.

[12]Shkarayev, S., Jouse, W., Null, W., and Wagner, M., "Measurements and Performance Prediction of an Adaptive Wing Micro Air Vehicle," *Smart Structures and Materials 2003: Industrial and Commercial Applications of Smart Structures Technologies*, edited by Eric H. Anderson, Proceedings of SPIE, Vol. 5054, International Society for Optical Engineering, Bellingham, WA, 2003, pp. 53–65.

[13]Selig, M. S., Lyon, C. A., Giguère, P., Ninham, C. N., and Guglielmo, J. J., "Summary of Low-Speed Airfoil Data," SoarTech Publications, Vol. 2, Virginia Beach, VA, 1996.

[14]Null, W., and Pereira, M., "Development of Surveillance and Endurance Micro Air Vehicles for the 2003 Micro Air Vehicle Competition," Report to the 7th International Micro Air Vehicle Competition, Univ. of Florida, Gainesville, FL, April 2003.

[15]Aki, M., and Noseck, A., "Calibration of Low Speed Wind Tunnel," AME Dept., Univ. of Arizona, Tucson, Aug. 2004.

[16]Kline, S. J., and McClintock, F. A., "Describing Uncertainties in Single-Sample Experiments," *Mechanical Engineering*, Vol. 75, No. 1, 1953, pp. 3–8.

[17]Barlow, J. B., Rae, W. H., Jr., and Pope, A., *Low-Speed Wind Tunnel Testing*, 3rd ed., Wiley, New York, 1999, p. 713.

[18]Waszak, M., Jenkins, L., and Ifju, P., "Stability and Control Properties of an Aeroelastic Fixed Wing Micro Aerial Vehicle," AIAA Paper 2001-4005, Aug. 2001.